Comparison between RINGSS and MASS-DIMM at Cerro Tololo

Authors:*A. Tokovinin*
Version: 1
Date: 2023-02-22
File: prj/atm/smass/test-feb2023/report-feb2023.tex

1 Introduction

The RINGSS turbulence profiler has been operating at Cerro Tololo in robotic mode since mid-November 2022. It is installed at 6 m height above ground on the Halfmann tower. A total of 46,129 turbulence measurements have been collected by February 15, 2023. The regular MASS-DIMM site monitor has been operational only part of this period owing to problems with its mount and pointing; it stopped on January 8, 2023 and was back in service after February 15. This document compares the data of two site monitors, RINGSS and MASS-DIMM, collected during simultaneous operation. A preliminary comparison based on several nights in August 2022 was reported earlier.[1].

2 Data scope and quality

1. MASS-DIMM. Data from the regular MASS-DIMM monitor for the period 2022-11-09 to 2022-02-15 have been downloaded from the web interface[2] as two test files with DIMM and MASS results. They contain 18,928 individual DIMM measurements with 1 min. cadence and 18,676 MASS measurements (turbulence profiles). Data from the text files were read into IDL structures using the codes `getsee.pro` and `getmass.pro`. Analysis of DIMM data shows a stable separation between spots (mean 52.8 pixels, rms scatter 2.52 pixels) and large Strehl ratios (mean 0.80 and 0.78 for the left and right spots, respectively). So, these data are accepted without any filtering.

2. RINGSS. Data from each night are collected in two text files with extensions `.stm` (statistical moments) and `.prof` (turbulence profiles). Each turbulence profile is determined from statistical moments averaged from ten 2-s data cubes. The measurement cadence is about 40 s. The files were copied from the instrument computer NUC1 (IP 139.229.13.65:6059) to the local disk. The IDL code `readprof.pro` reads both kinds of files into a structure `dat` that is used by the existing IDL programs for data management. A list of 58 dates is supplied (excluding nights with few RINGSS data), and all these nights are combined in one structure. The procedure `filterdat` removes obvious outliers using the following criteria: (i) ring radius within 5% from the mean, (ii) seeing less than $4''$, and (iii) rms error of profile restoration less than 0.3. The filtered structure contains 46,129 individual measurements. Note that although the IDL is used here for the data analysis, the data come from the RINGSS software written in python. For comparison with MASS-DIMM, RINGSS data where the average cube center was displaced by more than 6 pixels are excluded, leaving 41,630 points; in

[1] report-20221108.pdf
[2] http://139.229.13.222/web/CTIO/ctio_site_monitoring.php

the rejected data, some ring images can be truncated owing to guiding errors. The RINGSS seeing measurements from scintillation, `see`, are used for comparison with DIMM.

3. Data matching. The code `compare8.pro` matches the two data sets. For each RINGSS measurement, data from DIMM and MASS with time stamps within 1 min. are looked for and, if found, averaged. Almost all data are matched to RINGSS (18,901 for DIMM and 18,696 for MASS). The plots presented here are produced using this code.

3 Seeing comparison

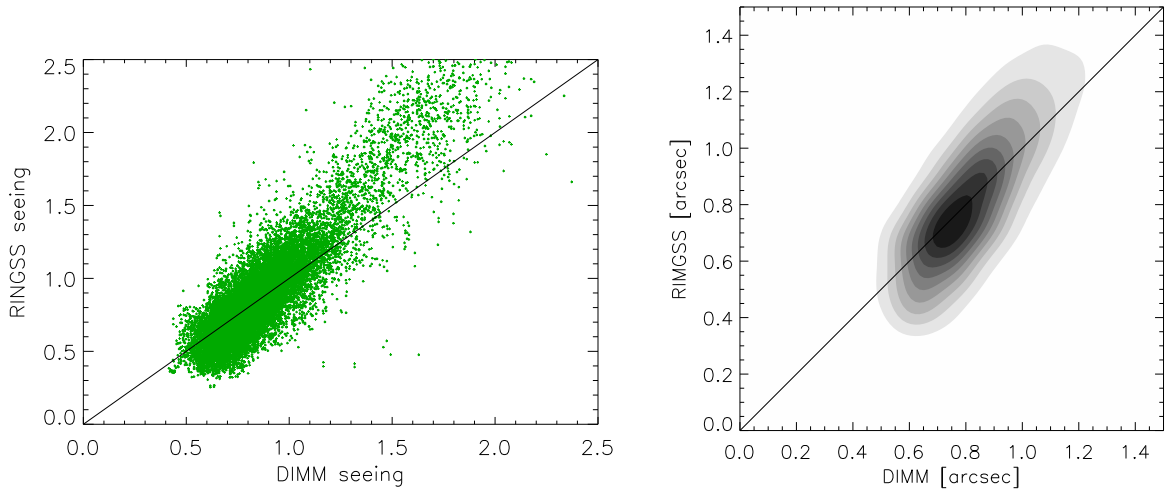

Figure 1: Comparison of the total seeing measured by RINGSS and DIMM. In both plots the diagonal corresponds to equality.

Overall, the seeing measured by DIMM and RINGSS agree very well. The mean and median ratios RINGSS/DIMM are both 1.02. The `see2` values are slightly larger, with the mean and median ratio of 1.07. Figure 1 presents the X-Y comparison in two forms: all points and the density plot. The linear regression is

$$\epsilon_{\rm RINGSS} = -0.274 + 1.355\epsilon_{\rm DIMM}. \qquad (1)$$

One notes that when the seeing is poor, RINGSS gives slightly larger values than DIMM. Figure 2 gives further insights. The left-hand plot illustrates how spikes of poor seeing are measured with a larger amplitude by RINGSS. The right-hand plot associates these "overshoots" with stronger scintillation, i.e. high-altitude turbulent layers. In these conditions the weak-turbulence approximation which underlines RINGSS data reduction becomes increasingly poor. The RINGSS software partially corrects for this effect using a simulation-based prescription, as in MASS. However, the DIMM seeing is not corrected for strong scintillation (DIMM implicitly assumes turbulence concentrated near the ground). Under strong scintillation, DIMM is expected to under-shoot owing to diffraction and partial saturation.

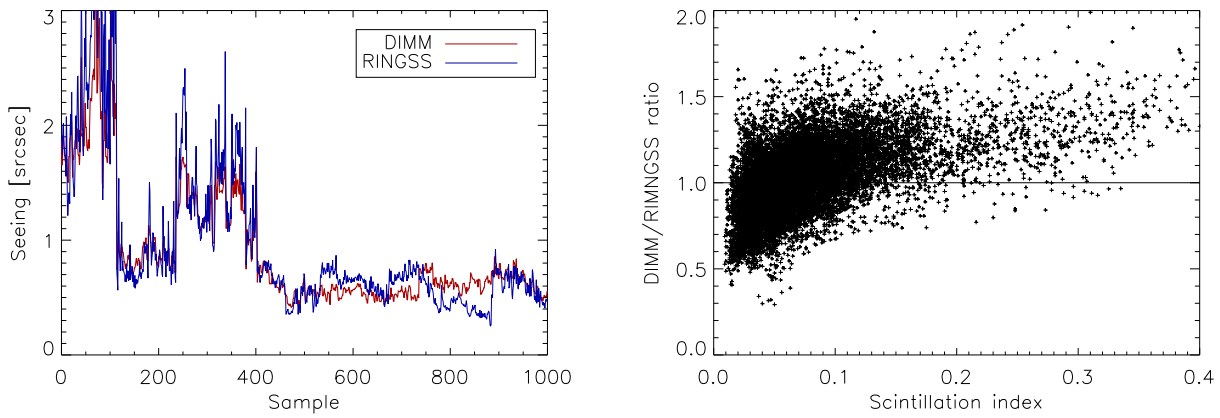

Figure 2: **Left:** seeing vs. sample number for the first 1000 matched points. **Right:** Ratio of RINGSS/DIMM seeing vs. scintillation index in RINGSS.

Figure 2 (left) also evidences "local" disagreements between RINGSS and DIMM under good (half-arcsecond) seeing. The two instruments diverge in both directions, albeit mildly. The reason could be differences in the viewing directions (different stars) and local turbulence neat each tower. The old DIMM is known to be affected by local turbulence generated near the edge of the Tololo platform, as evidenced by its comparison with the TMT DIMM (paper by S.Els et al.). Combination of local turbulence under good seeing and under-shoots at poor seeing posibly explains the slope of the formal linear regression.

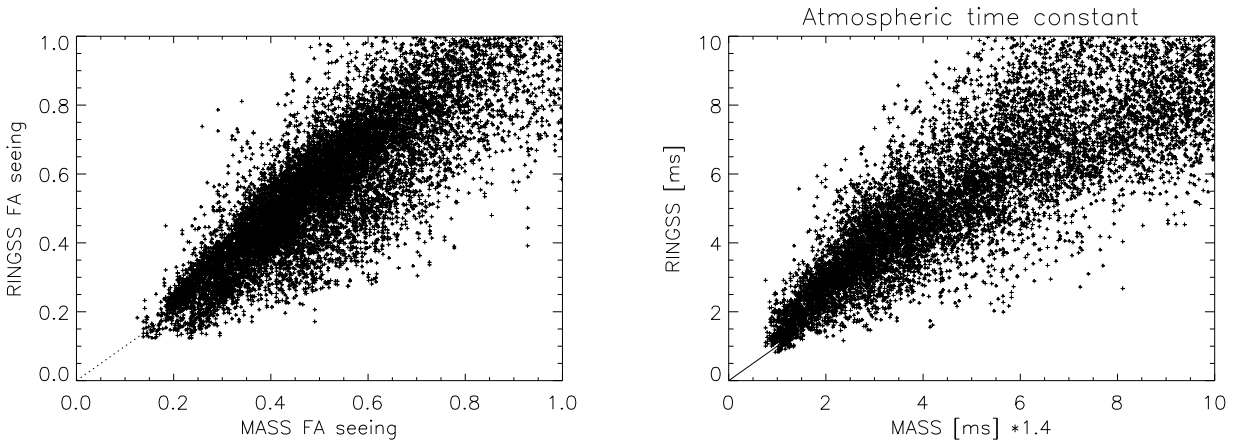

Figure 3: **Left:** Comparison of free-atmosphere seeing. **Right:** comparison of atmospheric time constants.

Figure 3 complements by comparing the MASS data products (free-atmosphere seeing and time constant τ_0) with RINGSS. For RINGSS, the FA seeing is computed by from the sum of turbulence integrals from 0.5 km up and adding half of the 0.25-km layer to better emulate MASS which does

not have the 0.25-km layer. The median and mean ratio of FA seeing RINGSS/MASS is 1.11. As for the time constant, it is known that the method implemented in MASS is very approximate and the results are biased.[3] The values of τ_0 reported by MASS with a corrective factor of 1.4 agree reasonable well with RINGSS.

4 Profile comparison

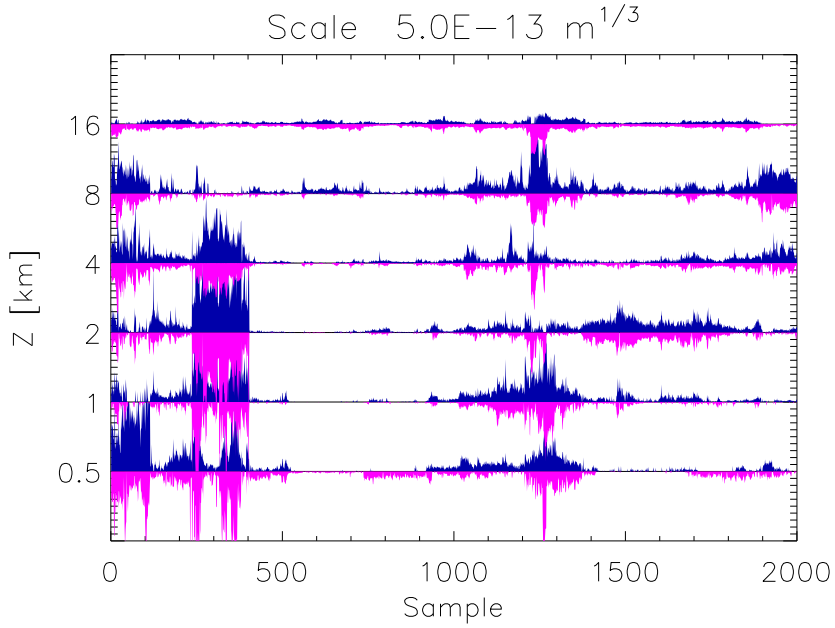

Figure 4: Turbulence integrals J in each layer vs. sample number. The RINGSS data are up-facing blue bars, MASS is plotted as down-facing magenta bars. Vertical interval between the lines corresponds to $J = 5\ 10^{-13}\ \mathrm{m}^{1/3}$.

Detailed comparison between turbulence profiles measured simultaneously by MASS and RINGSS reveals overall agreement and some systematic differences. Figure 4 illustrates the first 2000 matched samples in a semi-qualitative way. The turbulence spikes are localized by both instruments at consistent altitudes and with comparable amplitudes.

A detailed comparison for all six MASS layers is presented in Figure 5. The systematic difference appears in the highest layers, where RINGSS puts more turbulence in the 8-km layer and less in the 16-km layer, compared to MASS. This mismatch is also notable in Figure 4. It will be investigated further using simulations.

[3]Tokovinin, A. 2009. Calibration of the MASS time constant by simulation. http://www.ctio.noirlab.edu/ atokovin/profiler/timeconstnew.pdf

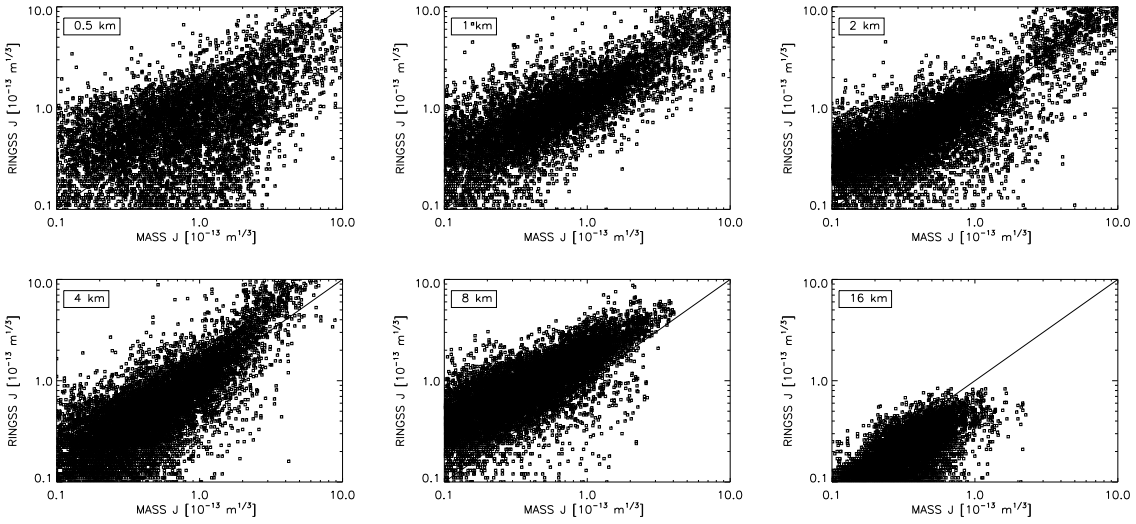

Figure 5: Comparison of turbulence integrals J layer by layer: MASS on the horizontal axis, RINGSS on the vertical axis. Logarithmic scale, the line is 1:1.

5 Conclusions

The comparison between RINGSS and MASS-DIMM shows a good agreement of integral parameters (total and FA seeing and atmospheric time constant). The DIMM slightly under-shoots under strong scintillation, as expected (it does not account for the second-order effects). A systematic difference of turbulence integrals in the 8-km and 16-km layers is found and requires further investigation.